CHIN. PHYS. LETT. Vol. 38, No. 1 (2021) 016801

Photonic Thermal Rectification with Composite Metamaterials

Ogundare Rasheed Toyin[1†], Wenxuan Ge(葛文宣)[1†], and Lei Gao(高雷)[1,2*]

[1]*College of Physical Science and Technology & Collaborative Innovation Center of Suzhou Nano Science and Technology, Soochow University, Suzhou 215006, China*
[2]*Jiangsu Key Laboratory of Thin Films, Soochow University, Suzhou 215006, China*

(Received 26 September 2020; accepted 2 December 2020; published online 6 January 2021)

We demonstrate strong photonic thermal rectification effect between polar dielectrics plate and the composite metamaterials containing nonspherical polar dielectric nanoparticles with small volume fractions. Thermal rectification efficiency is found to be adjusted by the volume fractions and the nanoparticles' shape, and it can be as large as 80% when the polar dielectric nanoparticles are spherical in shape and are in the dilute limit with the volume fraction $f = 0.01$. Physically, there exists strong electromagnetic coupling between the surface phonon polariton mode of polar dielectrics plate and the localized surface phonon polariton mode around polar dielectric nanoparticles. The results provide alternative new freedom for regulating energy flow and heat rectification efficiency in the near field, and may be helpful for design of multiparameter adjustable thermal diodes.

DOI: 10.1088/0256-307X/38/1/016801

Recently, there appears to be a new field called thermotronics based on the development of near-field radiative heat transfer (NFRHT) and other thermal fields such as far-field radiation with focus on thermal current instead of electrical ones.[1] When a thermal diode is applied with different temperature gradients in forward or reversed direction between two points, it would result in asymmetric heat fluxes.[1] The strength of manipulating heat flow led to various achievements of thermal component such as data storage devices,[2] thermal diodes,[3–8] nanophotonic thermal devices,[9,10] thermal transistor,[1,11,12] and thermal memories.[13,14] Considering thermal diodes to a large extent, asymmetric devices using heat conduction[15] and far-field heat radiation[16,17] are relatively convenient to manufacture. However, NFRHT has more advantages in other aspects. Due to the tunneling of evanescent wave, devices based on NFRHT can realize a very high degree of integration. In addition, this type of thermal diodes can also be based on a variety of physical mechanisms, with a high degree of control. Specifically, NFRHT can be enhanced significantly by the coupling between surface phonon polaritons (SPhPs) or surface plasmon polaritons (SPPs), which promotes its significant usefulness in energy conversion systems.[18–20] For instance, Otey *et al.*[21] proposed to tune the near-field heat exchange using two plates, and a rectification coefficient of 0.41 was envisaged as the maximum. This was due to altering the temperature of optical properties of the materials. Afterward, Lizuka and Fan[3] investigated the thermal rectification between temperature set of 500 K and 300 K using a SiC-coated dielectric plate, and obtained the maximal thermal rectification efficiency of 0.44. Tang *et al.*[5] was first to extend this area of investigation using planar thermal diodes of the same materials, and achieved the maximal rectification coefficient of 0.63. On the other hand, engineering composite metamaterials has become an essential tool[22–24] to modify materials' properties physically from macroscale to mesoscale. By replacing the permittivity of one material with another, the NFRHT can be modified.[25] Previous theoretical and experimental studies on tip–plate,[26,27] sphere–plate[28,29] and plate–plate[30] configurations revealed that the separation distance and the dielectric properties can be adopted to control the NFRHT. The NFRHT at the nanoscale[31,32] can be tuned in other ways using composites or phase change materials.[33–35]

In this Letter, we study theoretically the NFRHT between a semi-infinite 3C-SiC plate and a semi-infinite composite metamaterial plate containing nonspherical 3C-SiC particles with the volume fraction f randomly suspended in the host medium, separated by gap d as depicted in Fig. 1. The two plates are maintained respectively at different temperatures $T_{\rm L}$ and $T_{\rm H}$ ($T_{\rm H} > T_{\rm L}$) corresponding to the receiver's and emitter's temperatures, respectively. The relative permittivity for the 3C-SiC is given by[36]

$$\varepsilon_1(\omega, T) = \varepsilon_\infty\left(1 - \frac{\omega_{\rm LO}^2 - \omega_{\rm TO}^2}{\omega^2 - \omega_{\rm TO}^2 + i\Gamma\omega}\right), \tag{1a}$$

where $\varepsilon_{1\infty}$, Γ, $\omega_{\rm TO}$ and $\omega_{\rm LO}$ are the relative permittivity at high frequency, damping constant, the trans-

Supported by the National Natural Science Foundation of China (Grant Nos. 11774252 and 92050104), the Qing Lan Project, and the PAPD of Jiangsu Higher Education Institutions.
†Ogundare Rasheed Toyin and Wenxuan Ge contributed equally to this work.
*Corresponding author. Email: leigao@suda.edu.cn

verse and longitudinal phonon frequencies,

$$\varepsilon_{1\infty} = 6.7\exp[5\times10^{-5}(T-300)], \quad (1b)$$
$$\omega_{\rm LO} = 182.7\times10^{12} - 5.463\times10^{9}(T-300), \quad (1c)$$
$$\omega_{\rm TO} = 149.5\times10^{12} - 4.106\times10^{9}(T-300), \quad (1d)$$
$$\Gamma = 6.6\times10^{11}\left[1+\frac{2}{\exp[\hbar\omega_{\rm TO}/k_{\rm B}T]-1}\right]. \quad (1e)$$

For the composite metamaterial plate, its effective permittivity can be expressed in the generalized Maxwell-Garnett approximation[37] as follows:

$$\varepsilon_{\rm e} = \frac{f\varepsilon_1\beta + (1-f)\varepsilon_2}{f\beta + 1 - f}, \quad (2)$$

where $\beta = \frac{1}{3}\sum_{j=x}^{z}\varepsilon_2/[L_j\varepsilon_1 + (1-L_j)\varepsilon_2]$ is the field factor, ε_1 and ε_2 are the relative permittivity of the 3C-SiC and the host medium. We assume that SiC particles are ellipsoidal in shape, characterized by the depolarization factors L_x, L_y, and L_z satisfying the sum rule[38] $L_x + L_y + L_z = 1$. To elucidate further, we assume all ellipsoids to be spheroidal in shape with the symmetry towards the z axis, $L_x = L_y$. For a given L_z, we have $L_x = L_y = (1-L_z)/2$.

In the present system, the effective permittivity is adopted to calculate the spectral heat function and the rectification efficiency. For our model, both the volume fraction and depolarization factor can be adjusted simultaneously, and hence can be used to control the rectification factor, resulting in high rectification coefficient.

Without loss of generality, the top plate is in forward-biased scenario with temperature $T_{\rm H}$ and radiative heat flux $Q_{\rm f}$ while it is at reverse scenario with low temperature $T_{\rm L}$ and radiative heat flux $Q_{\rm r}$. Thermal diode performance is characterized by the rectification efficiency[6,39]

$$\eta = \frac{|Q_{\rm f} - Q_{\rm r}|}{\max(Q_{\rm f}, Q_{\rm r})}. \quad (3)$$

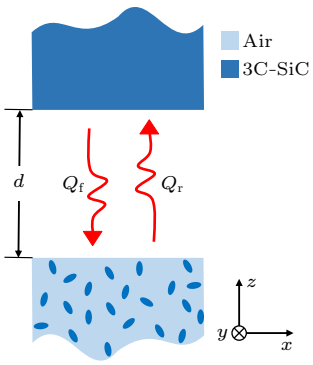

Fig. 1. Diagram of NFRHT between two plates separated by gap d with the upper plate at temperature $T_{\rm H}$ in the forward-bias case while it maintains a low temperature $T_{\rm L}$ in the reverse-bias case, also the lower plate at temperature $T_{\rm L}$ in the forward-bias case while it maintains a high temperature $T_{\rm H}$ in the reverse-bias case.

The net heat flux can be written as[39]

$$Q = \int_0^\infty q_\omega d\omega = \frac{1}{4\pi^2}\int_0^\infty d\omega\left[\Theta(\omega,T_{\rm H}) - \Theta(\omega,T_{\rm L})\right] \cdot \int_0^\infty \beta d\beta \sum_{\alpha=s,p}\tau_\alpha(\omega,\beta,d), \quad (4)$$

where $\Theta(\omega,T) = \hbar\omega/2[\coth(\hbar\omega/2k_{\rm B}T)]$ is the Planckian function, β is the parallel wave vector, and q_ω is called the net spectral heat function. In addition, τ_α (sum over s and p polarizations) is the total energy transmission factor which includes the contributions from both propagating wave ($\beta < k_0$) and evanescent wave ($\beta > k_0$) in the NFRHT, and admits the form[39]

$$\tau_\alpha(\omega,\beta,d) = \frac{(1-|r_{1\alpha}|^2)(1-|r_{2\alpha}|^2)}{|1-r_{1\alpha}r_{2\alpha}e^{2i\kappa d}|^2}, \quad \beta < \omega/c,$$
$$\tau_\alpha(\omega,\beta,d) = \frac{4{\rm Im}(r_{1\alpha}){\rm Im}(r_{2\alpha})e^{-2{\rm Im}(\kappa)d}}{|1-r_{1\alpha}r_{2\alpha}e^{-2{\rm Im}(\kappa)d}|^2}, \quad \beta > \omega/c, \quad (5)$$

where $r_{1\alpha}$ and $r_{2\alpha}$ are the Fresnel reflection coefficients.

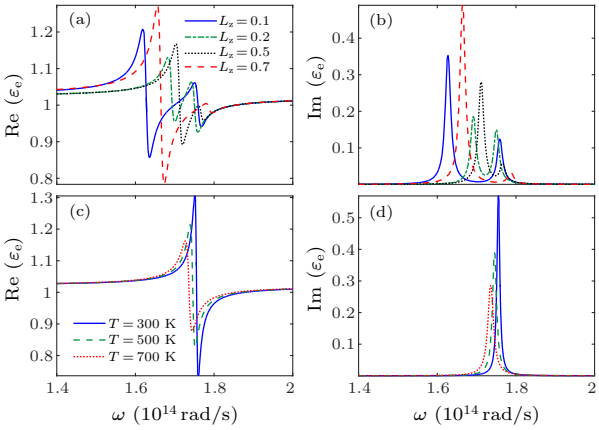

Fig. 2. Real part (a) and imaginary part (b) of $\varepsilon_{\rm e}$ against ω with $f = 0.01$ at temperatures $T = 700$ K for different L_z. Real part (c) and imaginary part (d) of $\varepsilon_{\rm e}$ against ω at $L_z = 1/3$ for different temperatures.

In order to confirm the quantitative results for thermal rectification, we first investigate the effective permittivity ($\varepsilon_{\rm e}$) of the composite metamaterials as a function of the angular frequency for $f = 0.01$, as shown in Fig. 2. From Figs. 2(a) and 2(b), it is evident that both the real part and the imaginary part exhibit two peaks for different values of L_z in the ellipsoidal shape (except for $L_z = 0.3$, which is close to the spherical shape). The peaks result from the localized surface phonon polariton (LSPhP) modes, whose frequencies can be quantitatively determined by the relation $L_i{\rm Re}(\varepsilon_1) + (1-L_i)\varepsilon_2 = 0$ along $i = x$ or $i = z$ axis. On the other hand, the real part of the effective permittivity is positive and above zero. This clarifies the fact that no SPhP mode takes place at the surface

of the composite metamaterials. For the composite metamaterials containing spherical nanoparticles, one single resonant peak arises, and the increase of temperature leads to the decrease of the peak magnitude accompanied with the red shift of the resonant peak, as shown in Figs. 2(c) and 2(d). Also, it is observed that the effective permittivity (ε_e) of the composite metamaterials with spherical particles is analogous to the permittivity of SiC[36,40] except that the values are small. This shows the effect of the effective medium theory on the effective permittivity.

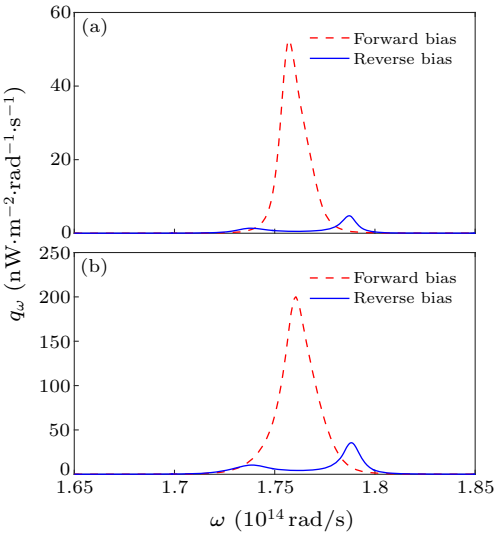

Fig. 3. Values of q_ω as a function of ω for the forward- and reverse-bias cases at $T_L = 300$ K and $T_H = 700$ K. The volume fraction used are (a) 0.01 and (b) 0.1 respectively.

In order to understand the physical mechanism of thermal rectification between the 3C-SiC plate and the composite metamaterials' plate containing spherical 3C-SiC nanoparticles, we plot the variation of q_ω with ω in Fig. 3 for a vacuum gap of 30 nm. From Fig. 3(a), one observes that the net spectral heat flux in the forward biased scenario achieves the peak enhancement at the frequency $\omega = 1.757\times10^{14}$ rad/s and in the reverse biased scenario, there are two small resonant peaks at $\omega = 1.747\times10^{14}$ rad/s and $\omega = 1.787\times10^{14}$ rad/s. As one knows, the 3C-SiC plate possesses one surface phonon polariton frequency $\omega_{\rm SPhP}(T)$ at $\mathrm{Re}[\varepsilon_1(T)] + 1 = 0$, while the composite metamaterials containing spherical SiC nanoparticles have one LSPhP resonant frequency $\omega_{\rm LSPhP}(T)$ at $\mathrm{Re}[\varepsilon_1(T)] + 2 = 0$. In the forward-bias case, the resonant frequency for SPhP coincides with the one for LSPhP, i.e., $\omega_{\rm SPhP}(T = 700\,\mathrm{K}) \approx \omega_{\rm LSPhP}(T = 300\,\mathrm{K})$, and hence the interaction between the SPhP and LSPhP modes is strong, resulting in one enhancement peak. On the contrary, for the reverse-bias case, $\omega_{\rm SPhP}(T = 300\,\mathrm{K})$ is separated from $\omega_{\rm LSPhP}(T = 700\,\mathrm{K})$, and the interaction between the two modes becomes weaker. As a consequence, one observes two small peaks. Such a difference between the forward- and reverse-bias scenarios indicates the heat rectification, which will be further discussed in the following. For a large volume fraction [see Fig. 3(b)], we can obtain a large net spectral heat function. According to our calculation, the p-polarized wave contributes more to the spectral heat flux in the forward-bias case as compared to the s-polarized wave which is trifling in both the cases.

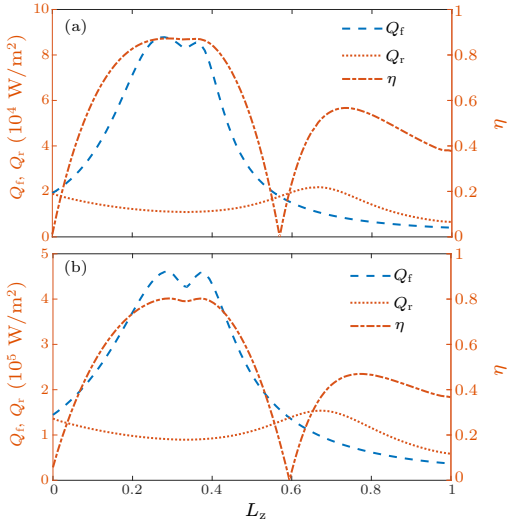

Fig. 4. Effect of volume fraction on rectification efficiency (vertical right axis) in relation to total heat flux parameters as a function of the depolarization factor (a) $f = 0.01$ and (b) $f = 0.1$, at $T_L = 300$ K and $T_H = 700$ K.

In Fig. 4 we investigate the effect of nanoparticles' shape on the heat flux and rectification efficiency. For small volume fraction such as $f = 0.01$, strong forward heat flux is found around $L_z = 1/3$ (3C-SiC nanoparticles are spherical in shape), while the reverse heat flux is weak. The contrast between them indicates strong rectification efficiency of larger than 80%. For large volume fraction such as $f = 0.1$ [see Fig. 3(b)], although both the forward and reverse heat fluxes become relatively larger, the rectification efficiency is still less than 80%. Therefore, small volume fraction of spherical nanoparticles in composite metamaterials is quite helpful for enhancement of the rectification efficiency.

In Fig. 5, we present the contour plot for the energy transmission factor, i.e. the net spectral heat flux per unit interval of $\beta c/\omega$. There is little or insignificant heat flow for $\beta c/\omega < 1$ (propagating wave), and heat flow exists in the range $\beta c/\omega > 1$ (evanescent wave). For $f = 0.01$, $\mathrm{Re}(\varepsilon_e) > 0$, the composite metamaterials do not support the SPhP mode but there exists the LSPhP mode, which occurs at $\mathrm{Re}(\varepsilon_1) = -2$. The dashed green lines and dashed red lines shown in Figs. 5(a) and 5(b), respectively, depict that the SPhP mode is supported by the 3C-SiC plate at the resonant frequency $\omega_{\rm SPhP}$ and the LSPhP mode is supported by the 3C-SiC nanoparticles at a resonant frequency $\omega_{\rm LSPhP}$. For the forward scenario, the coupling between SPhP mode and LSPhP modes is strong, leading to relatively larger Q_f. For the reverse-bias case,

the resonant frequency of the LSPhP mode is far from that of the SPhP mode, so Q_r is quite small. This results in a higher rectification efficiency. The similar analysis is also applicable to the case of $f = 0.1$.

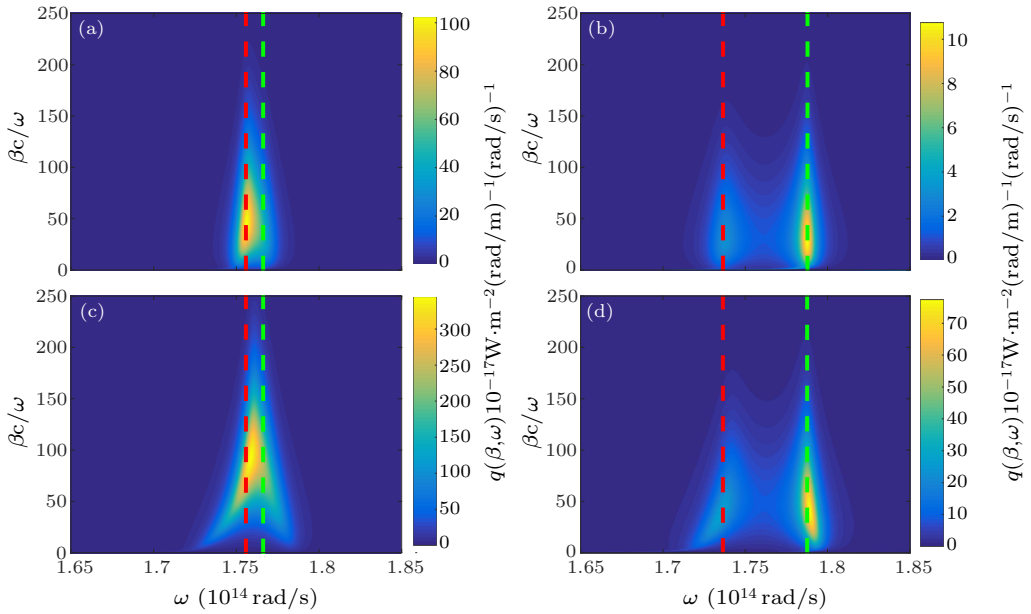

Fig. 5. Energy transmission plots for the forward scenarios: with $L_z = 1/3$ for (a) $f = 0.01$ and (c) $f = 0.1$, and reverse scenarios: with $L_z = 1/3$ for (b) $f = 0.01$ and (d) $f = 0.1$, at $T_L = 300$ K and $T_H = 700$ K.

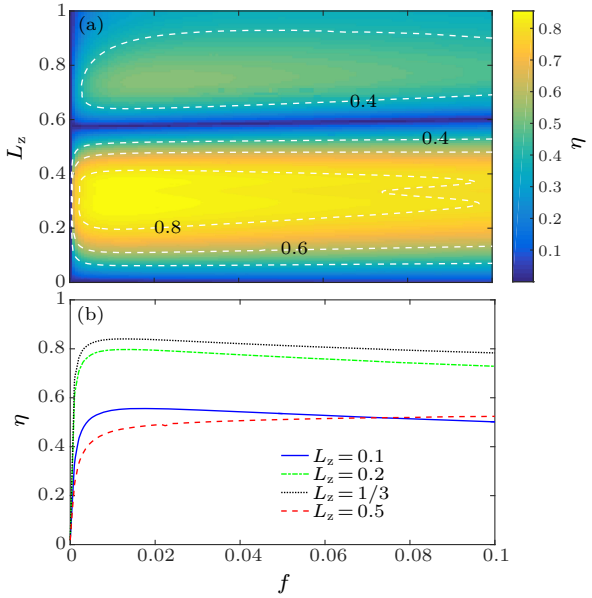

Fig. 6. Different L_z values for the rectification efficiency against volume fraction, for $T_L = 300$ K and $T_H = 700$ K.

As shown in Figs. 3–5, the volume fraction and the depolarization factor have greater effects on the heat flux and the rectification efficiency. To elucidate further, we plot the graph of rectification efficiency against f in Figs. 6 for various depolarization factors. We observe an optimal volume fraction $f_{op} = 0.01$ satisfying the maximal rectification efficiency for $L_z = 1/3$. This can simply be understood as follows: by tuning volume fraction, the resonant frequency of the LSPhP mode on the composite metamaterials keep variant, while the SPhP mode of 3C-SiC plate remains unchanged. Strongest overlapping between the SPhP mode of pure 3C-SiC plate and the LSPhP mode around the 3C-SiC nanoparticles in the composite metamaterials requires the *optimal volume fraction*, and hence attain the peak of heat flux.

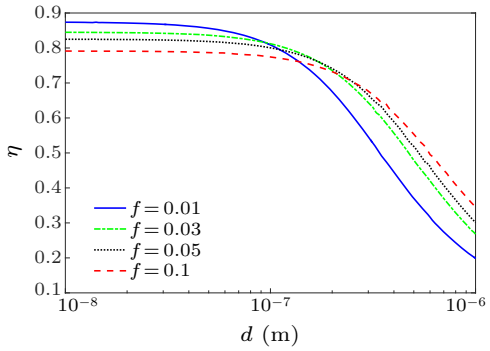

Fig. 7. Different f values for the rectification efficiency against vacuum gap, at $T_L = 300$ K and $T_H = 700$ K.

Furthermore, we plot the graph of the thermal rectification efficiency against the gap d in Fig. 7 for the values of $f = 0.01$, 0.03, 0.05 and 0.10, respectively. In the cases of volume fraction $f = 1/3$ or smaller, the rectification efficiency is enhanced drastically. Under these conditions, over 50% efficiencies can be maintained for $d = 100$ nm or smaller with $L_z = 1/3$. These actually conform the results obtained in Fig. 6. Higher efficiency can be obtained as d reduces. For instance, a volume fraction of $f = 0.01$ at $d = 10$ nm yields an efficiency of almost 85%, which implies the optimal volume fraction discussed in Fig. 6 and it corresponds to the efficiency as shown in Fig. 4(a), respectively. Finally, Fig. 8 depicts the plot of rectification efficiency against the high temperature T_H for volume

fractions of interest, keeping $T_{\rm L} = 300\,{\rm K}$. From Fig. 8, we can see that the rectification efficiency increases monotonically with increasing $T_{\rm H}$, and a volume fraction of $f = 0.01$ gives the highest rectification efficiency, which corresponds to the other results as discussed above.

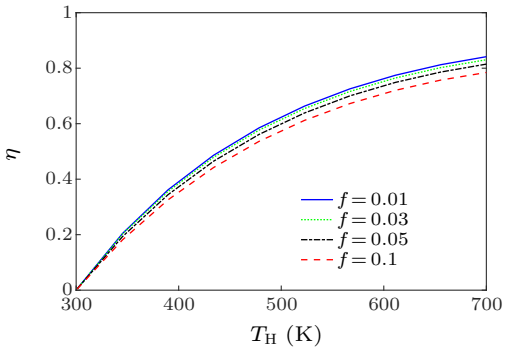

Fig. 8. The rectification efficiency against high temperature $T_{\rm H}$ for different f values at $L_z = 1/3$ and $T_{\rm L} = 300\,{\rm K}$.

In conclusion, we have proposed a photonic thermal rectifier based on composite metamaterials. Large thermal rectification efficiency above 80% is predicted when the composite metamaterials are composed of small volume fraction of spherical nanoparticles randomly embedded in the host medium. The physical mechanism is attributed to the strong/weak coupling between the SPhP mode of the 3C-SiC plate and the LSPhP mode of composite metamaterials containing 3C-SiC nanoparticles in the forward- and reverse-bias scenarios. Beyond their potentials for thermal management, the photonic thermal rectifiers based on the composite metamaterials may suggest the possibility to develop photonic thermal transistors and thermal memories for processing information.

References

[1] Prod'homme H, Ordonez-Miranda J, Ezzahri Y, Drevillon J and Joulain K 2018 *J. Quant. Spectrosc. Radiat. Transfer* **210** 52
[2] Ghanekar A, Tian Y P, Ricci M, Zhang S, Gregory O and Zheng Y 2018 *Opt. Express* **26** A209
[3] Iizuka H and Fan S H 2014 *J. Quant. Spectrosc. Radiat. Transfer* **148** 156
[4] Xu G, Sun J, Mao H and Pan T 2019 *J. Quant. Spectrosc. Radiat. Transfer* **232** 20
[5] Tang L and Francoeur M 2017 *Opt. Express* **25** A1043
[6] Wang H, Hu S, Takahashi K, Zhang X, Takamatsu H and Chen J 2017 *Nat. Commun.* **8** 15843
[7] Wang L P and Zhang Z M 2013 *Nanoscale Microscale Thermophys. Eng.* **17** 337
[8] Wang K Y and Gao L 2020 *ES Energy & Environ.* **7** 12
[9] Philippe B A and Svend-Age B 2014 *Phys. Rev. Lett.* **112** 044301
[10] Lo W C, Wang L and Li B 2008 *J. Phys. Soc. Jpn.* **77** 054402
[11] Lenert A, Bierman D M, Nam Y, Chan W R, Celanovic I, Soljacic M and Wang E N 2014 *Nat. Nanotechnol.* **9** 126
[12] Challener W A, Peng C, Itagi A V, Karns D, Peng W, Peng Y, Yang X, Zhu X, Gokemeijer N J, Hsia Y T, Ju G, Rottmayer R E, Seigler M A and Gage E C 2009 *Nat. Photon.* **3** 220
[13] Ghanekar A, Ricci M, Tian Y P, Gregory O and Zheng Y 2018 *Appl. Phys. Lett.* **112** 241104
[14] Yang Y and Wang L P 2017 *J. Quant. Spectrosc. Radiat. Transfer* **197** 68
[15] Chang C W, Okawa D, Majumdar A and Zettl A 2006 *Science* **314** 1121
[16] Jia S C, Fu Y, Su Y S and Ma Y G 2018 *Opt. Lett.* **43** 5619
[17] Kasali S O, Ordonez-Miranda J and Joulain K 2020 *Int. J. Heat Mass Transfer* **154** 119739
[18] Whale M D and Cravalho E G 2002 *IEEE Trans. Energy Convers.* **17** 130
[19] Laroche M R, C and Greffet J J 2006 *J. Appl. Phys.* **100** 063704
[20] Park K, Basu S, King W P and Zhang Z M 2008 *J. Quant. Spectrosc. Radiat. Transfer* **109** 305
[21] Otey C R, Lau W T and Fan S 2010 *Phys. Rev. Lett.* **104** 154301
[22] Wang M and Pan N 2008 *Mater. Sci. Eng. R* **63** 1
[23] Balazs A C, Emrick T and Russell T P 2006 *Science* **314** 1107
[24] Krokhin A A, Arriaga J, Gumen L N and Drachev V P 2016 *Phys. Rev. B* **93** 075418
[25] Perez-Rodriguez J E, Pirruccio G and Esquivel-Sirvent R 2019 *Phys. Rev. Mater.* **3** 015201
[26] Kittel A, Wischnath U F, Welker J, Huth O, Rueting F and Biehs S A 2008 *Appl. Phys. Lett.* **93** 193109
[27] Worbes L, Hellmann D and Kittel A 2013 *Phys. Rev. Lett.* **110** 134302
[28] Shen S, Mavrokefalos A, Sambegoro P and Chen G 2012 *Appl. Phys. Lett.* **100** 233114
[29] Guha B, Otey C, Poitras C B, Fan S and Lipson M 2012 *Nano Lett.* **12** 4546
[30] Zhou C, Zharig Y, Yi H and Qu L 2019 *PhotonIcs & Electromagnetics Research Symposium-Spring* (Rome, Italy 17–20 June 2019) p 2652
[31] Shen S, Narayanaswamy A and Chen G 2009 *Nano Lett.* **9** 2909
[32] Yazmin S E and Esquivel-Sirvent R 2017 *Z. Naturforsch. A: Phys. Sci.* **72** 129
[33] Van Zwol P J, Ranno L and Chevrier J 2012 *Phys. Rev. Lett.* **108** 234301
[34] Jordan T H 2015 *Geophys. J. Int.* **203** 1343
[35] Choy T C 2016 *Effective Medium Theory Principles and Applications* (Oxford: Oxford Science Publications) vol 2 p 240
[36] Zhu L, Otey C R and Fan S 2013 *Phys. Rev. B* **88** 184301
[37] Gao L and Li Z 2003 *J. Phys.: Condens. Matter* **15** 4397
[38] Gao L, Wan J T K, Yu K W and Li Z Y 2000 *J. Phys.: Condens. Matter* **12** 6825
[39] Joulain K, Ezzahri Y, Drevillon J, Rousseau B and Meneses D D S 2015 *Opt. Express* **23** A1388
[40] Xu G, Sun J, Mao H and Pan T 2018 *J. Appl. Phys.* **124** 183104